First publ. in: Chemical Communications 46 (2010), 47, pp. 8939-8940, DOI: 10.1039/C0CC03364B

A modular approach towards functional decoration of peptide–polymer nanotapes†

Andreas Verch,[a] Harald Hahn,[a] Eberhard Krause,[b] Helmut Cölfen[ac] and Hans G. Börner*[ad]

DOI: 10.1039/c0cc03364b

Self-assembled peptide–polymer nanotapes of poly(ethylene oxide)–peptide conjugates are modified by a simple amine–azide transfer to create azide-containing nanofibres, which provide a platform for modular functionalization as demonstrated by the introduction of different carboxyl bearing entities to modulate the calcium binding properties of the nanotapes.

The utilization of functional, fibrillar nanostructures is a widespread concept, found in various biological processes to generate hierarchical composite materials such as bone, wood or glass sponge spicules.[1] Precisely positioned functionalities on fibrillar scaffolds serve multiple purposes in nature such as (i) control of partitioning of precursors in the early material constitution phase, (ii) compatibilization of constituents, and (iii) stabilization of mechanical interfaces. Recent advances in biomimetic design of fibre-guided or fibre-reinforced materials make means to fibrillar nanostructures with defined functional surfaces mandatory.[2]

Peptides proved to be highly suitable to generate anisotropic nanostructures with adjustable dimensions and precisely positioned functionalities.[3] Besides using the α-helical secondary structure motif,[4] particularly the β-sheet motif was studied intensively to program self-assembly of peptides, peptide–amphiphiles, peptide–polymer conjugates or protein–polymer conjugates.[5] The directional β-sheet assembly allows for the formation of anisometric nanostructures such as cylinders, tubes, tapes, fibrils or fibres.[6,7]

Previously, a peptide–polymer conjugate was described, which assembled into non-twisted β-sheet tapes (Fig. 1).[8] The bioconjugate was composed of a poly(ethylene oxide)-block (PEO) and a peptide segment. The latter consists of two short peptide sequences (5 mers), which were preorganized by an organic template based on 2,8-substituted carbazole.[8] The 9-amino functionality of the carbazole makes the coupling of a PEO block feasible. It has been demonstrated that multimers of a threonin-valine diade ($[TV]_x$) have a high β-sheet propensity and form stable assemblies in water or organic solvents if x equals 4–6.[7,9] The utilization of a carbazole template enhances the aggregation tendency, allowing shorter *dm*G–$(TV)_2$ peptides to assemble into stable β-sheets (*dm*G denotes *N*,*N*-dimethylglycine). The resulting tapes exhibited functional faces on which the cationic termini of the *dm*G and β-hydroxyl groups of threonine were presented. It has been evidenced that the functional nanoobjects mimicked some aspects of silica morphogenesis proteins.[10] Hence, the nanotapes could take part in a hybrid process to form complex silica composites with six levels of structural hierarchy.[11]

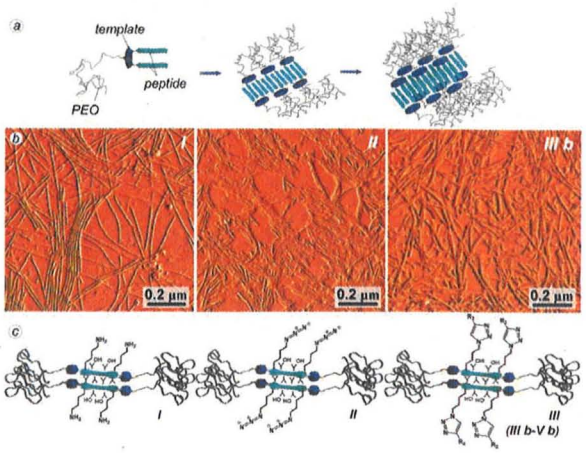

Fig. 1 (a) Schematic illustration of the self-assembly of a PEO–peptide conjugate *via* β-sheet tapes to nanotapes with double β-sheets (from left to right). (b) AFM micrographs of functional nanofibres, exhibiting amine—(I), azide—(II) and functional 1,2,3-triazole moieties (III b) and (c) the illustration of the side views of functional nanotapes (I, II and III).

Here, we present our efforts to develop a versatile strategy to decorate self-assembled peptide–polymer nanotapes with diverse functionalities in a post-modification step. As a result a modular tool box towards functional structures gets available, enabling one to introduce different functionalities onto preformed fibrillar scaffolds. Such a modular strategy appears to be advantageous compared to the direct assembly of newly synthesized functional building blocks. Besides demanding synthetic efforts, some functional residues might even interfere with the self-assembly process and hamper the formation of the targeted soft-matter structures.

Understanding the self-assembly of peptide–polymer conjugates allows for the rational introduction and positioning of functionalities in fibrillar nanostructures. A template preorganized PEO–peptide conjugate was synthesized by solid-phase supported peptide synthesis. The C-terminal extension of a *dm*G–$(TV)_2$ aggregator domain with lysine-valine leads to the [*dm*G–TVTVKV]$_2$–template–PEO conjugate (Scheme 1, I). This exhibits two ε-amino groups directed to the polar side of the peptide β-strands. The additional amino

[a] *Max Planck Institute of Colloids and Interfaces, Am Mühlenberg 1, D-14476 Potsdam, Germany*
[b] *Leibniz Institute of Molecular Pharmacology, Robert-Rossle-Str. 10, 13125, Germany*
[c] *University of Konstanz, Physical Chemistry, Universitätsstr. 10, D-78457 Konstanz, Germany*
[d] *Humboldt-Universität zu Berlin, Institute of Chemistry, Laboratory of Organic Synthesis of Functional Systems, Brooke-Taylor-Str. 2, D-12489 Berlin, Germany. E-mail: h.boerner@hu-berlin.de; Fax: +49 (0)30-20936919; Tel: +49 (0)30-20937348*
† Electronic supplementary information (ESI) available: Experimental data and methods. See DOI: 10.1039/c0cc03364b

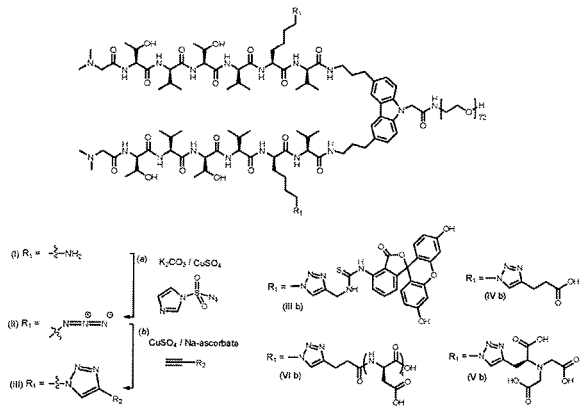

Scheme 1 Chemical structure of the PEO–peptide conjugate (top) and sequential functionality transformation by Cu^{2+} catalyzed diazo transfer (I → II) followed by click reaction (II → III) leading to functional bioconjugates (*conditions*: (a, b) H_2O, 12 h, rt).

acids do not interfere with the self-assembly process in water. Fig. 1(b I) depicts the fibrillar nanotapes that could be obtained by a sequential denaturation–reassembly procedure. The fibrils are several hundreds of nanometre in length, have widths of ~15.5 nm and heights of ~1.69 nm. The structural dimensions are analogous to those of previously observed nanotapes, which have been assembled from congener PEO–peptide conjugates.[8] Circular dichroism (CD) spectroscopy confirms that the peptides adopt a β-sheet by showing the typical cotton effects with a maximum at 196 nm and a minimum at 218 nm. Selected area electron diffraction indicates a β-strand spacing of d = 4.7 Å. Therefore, the inner structure of the nanotapes can be rationalized as a β-sheet ribbon (Fig. 1). The peptide segments of the bioconjugates assemble into extended β-sheets. The packing of the side chains of alternating polar–nonpolar amino acids generates a tape with facial amphiphilicity, where hydrophobic valine side chains are grouped on one side and polar threonine/lysine side chains are positioned on the opposing side. Two amphiphilic β-sheets are stacking to a double tape with a hydrophobic core and PEO-chains packed laterally.

As schematically shown in Fig. 1(c I), the ε-amino functionalities of the lysine residues are positioned at both sides of the ribbon, generating functional faces. The distinct antiparallel β-sheet motif allows for the calculation of the spacing. Two lines of amino functionalities can be expected with a lateral spacing of ~1.8 nm. Within each line the functionality occurs longitudinal with ~0.9 nm repeats. The ε-amino functionalities are accessible from the water phase and thus prone to chemical transformation reactions. This was demonstrated by exchanging the amino groups to an azide functionality *via* a diazo transfer reaction.[12] The utilization of the non-explosive, long term stable imidazole-1-sulfonyl azide hydrochloride (IS-N_3) proved to be a straightforward means, which avoids the danger of the established acido trifluoro-methane reagents.[13] The direct transformation of the amino groups on self-assembled nanotapes proceeds in a clean manner in water. The sensitive, colorimetric Kaiser test indicates the absence of free primary amino groups and suggests quantitative conversion. Infrared (IR) spectroscopy shows the appearance of a strong azide band at υ = 2100 cm^{-1}. Quantitative transformation was confirmed by both MALDI-TOF mass spectrometry and NMR spectroscopy. Moreover, CD-spectroscopy suggests the integrity of the peptide β-sheet assembly and both AFM as well as transmission electron microscopy (TEM) visualized fibrillar objects (*cf.* ESI†).

The azide functionalized nanotapes (II) were subsequently used as a scaffold to be decorated with functionalities on demand. For that purpose, copper catalyzed click chemistry as a robust, tolerant route proved to be suitable.[14] To demonstrate the approach, alkynated fluorescein dyes (III a) have been ligated to the fibrillar scaffolds, leading to dye decorated nanotapes (III b). Copper catalyzed click ligation enabled the introduction of the dye with yields > 75%. The anti-symmetric valence vibration of the azide entity at υ = 2100 cm^{-1} vanished in the IR spectrum of III b. ^{1}H-NMR confirms the chemical structure of III b. The integral intensity of the resonances of Val compared to those of PEO and the dye confirmed the conversion of II into III b. CD, TEM and AFM of the product III b show preservation of the fibrillar β-sheet structures (*cf.* ESI†). Comparisons of the structural dimensions of the amine-, azide- and dye-functional nanofibres (I, II, III b (*cf.* Table S1, ESI†)) as obtained from AFM and TEM micrographs indicate no dramatic changes of height and width during the amine–azide-transfer. The attachment of the fluorescein dye leads to a minor increase in height from 1.7 nm to 2.2 nm (AFM) while the widths of the nanofibres remained rather constant ~14–16 nm (TEM). Moreover, confocal laser scanning fluorescence microscopy enabled to visualize bundles of the dye modified fibres (*cf.* Fig. S6, ESI†). It should be noted that the major fraction of the dye marked nanotapes is clearly below the resolution limit of the applied optical microscopy method, and hence only larger bundles of fibrils could be visualized.

To demonstrate the versatility of the approach, three moieties bearing different carboxylate functionalities have been used to decorate the polymer–peptide-nanotapes (Scheme 1). The attachment of either 4-pentynoic acid (IV a), or propargylglycine–nitrilotriacetic acid (Pra–NTA, V a) or an alkyne functional (aspartic acid)$_6$ (alkyne-D_6, VI a) provides a set of functional nanotapes (IV b, V b and VI b). The click ligation proceeds with the three alkynes in a clean manner with rather good conversions. 4-Pentynoic acid as the smallest alkyne has been coupled nearly quantitatively according to IR and MALDI-TOF (*cf.* IV b, ESI†). The ligation of the more bulky Pra–NTA and alkyne-D_6 reached conversions of >85% as indicated by IR and NMR (*cf.* V b and VI b, ESI†). In all systems CD-spectroscopy suggests that the attachment of the alkynes does not disturb the peptide organization and AFM shows the preservation of the fibrillar nanostructures with lengths of up to several 100 nm (*cf.* ESI†).

In order to elucidate, if the different carboxyl functionalities have an effect on the nanotape properties, the modulation of calcium ion binding capabilities was investigated. The functional nanostructures IV b, V b and VI b were screened by calcium ion fingerprinting.[15] A Ca^{2+}-titration assay was applied, which allows for the determination of the calcium ion binding capability of the three different tapes (Fig. 2).

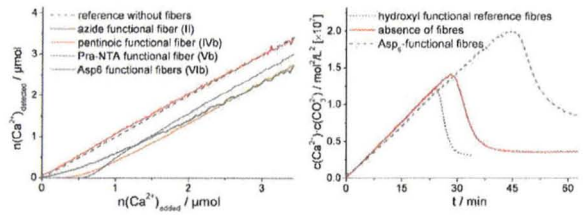

Fig. 2 Ca^{2+} fingerprinting (free Ca^{2+} in binding assays provides bound c[Ca^{2+}] as extrapolation of the linear stage to the *x*-axis (left) and crystallization inductor/retarder properties as evident from the development of the $CaCO_3$ ion product in the presence or absence of fibres (right)).

The functional decoration of the nanotapes clearly influences the ion interaction capability and allows the distinction between IV b, V b and VI b. A $CaCl_2$ solution was titrated to a solution of the fibres at a constant pH. The Ca^{2+} ion potential was monitored by means of an ion selective electrode. While the pentynoic acid modified nanotapes (IV b) bind 0.24 equiv. Ca^{2+} per COOH group, the nanotapes which have been decorated with the Pra–NTA derivative (V b) bind 0.12 equiv. Ca^{2+} per COOH group and the alkyne-$(D)_6$ modified nanofibres (VI b) bind 0.22 equiv. Ca^{2+} per carboxylate. These results can be rationalized by the conformational constrains of the different carboxylate bearing entities. As described in the literature NTA effectively complexes small ions *e.g.* Ni^{2+} or Fe^{3+}. To bind Ca^{2+} only two of three COOH groups are required. Probably, the compact geometry of the NTA-molecule prevents a reorientation of the COOH groups on the nanotapes, which leads to frustrated binding where not all COOH groups can be used effectively. Apparently, the pentynoic acid linked to the nanotapes is flexible enough to bind Ca^{2+} most effectively and the value of 0.24 equiv. Ca^{2+}/COOH is even superior to that of poly(acrylic acid) (0.21 Ca^{2+}/COOH).[15] The $(D)_6$ oligomers at the β-sheet tapes appear to be flexible enough to bind Ca^{2+} comparable to poly(acrylic acid). However, poly(aspartic acid) binds with 0.30 Ca^{2+}/COOH still more ions, which is probably due to the absence of end group effects.

Appropriate controls exclude that Ca^{2+} binding is dominated by the PEO–peptide scaffolds. Ca^{2+} fingerprinting with azido-functional nanotapes (II) or with PEO–peptide nanotapes of the [*dm*G–TVTV]$_2$–template–PEO[8] does not show significant Ca^{2+} binding (*cf.* Fig. 2).

In order to investigate the influence of the fibres on $CaCO_3$ nucleation, a crystallization assay was applied (Fig. 2, right). In this experiment, Ca^{2+} solution was dosed to a solution of the fibre in a carbonate containing buffer and the ion potential of free Ca^{2+} was monitored.[15,16] In all experiments the $CaCO_3$ ion product increased linearly prior to nucleation. However, the fibres show an influence on nucleation, which can be identified by the drop of the $CaCO_3$ ion product. Directly after nucleation, a phase is formed that is more soluble than amorphous calcium carbonate (ACC) as found in the reference experiment in the absence of fibres. In order to achieve a sufficient level of supersaturation, the $(D)_6$ decorated fibres inhibit the nucleation (by ~50%). Interestingly, the non-functional control (nanotapes of the [*dm*G–TVTV]$_2$–template–PEO) appears to promote nucleation compared to the reference experiments. This indicates a lowering of the activation barrier for nucleation possibly by heterogeneous nucleation on the fibres. Further investigations on the crystal morphologies obtained in the presence of functional fibres are in progress and will be reported elsewhere.

In conclusion, the present work demonstrates a modular approach to functional nanotapes. Self-assembled PEO–peptide nanotapes are modified by a diazo transfer reaction to introduce azide groups, to which alkynated functional entities could be ligated *via* click chemistry. The functionalization occurred under preservation of the nanostructures and was not disturbing the peptide organization.

This work was supported by the DFG (Emmy Noether BO1762/2) and Max Planck Society. We gratefully thank M. Antonietti, J. Brandt, and K. Ostwald.

Notes and references

1 J. N. Cha, K. Shimizu, Y. Zhou, S. C. Christiansen, B. F. Chmelka, G. D. Stucky and D. E. Morse, *Proc. Natl. Acad. Sci. U. S. A.*, 1999, **96**, 361; P. Fratzl, *Curr. Opin. Colloid Interface Sci.*, 2003, **8**, 32.
2 P. Fratzl and R. Weinkamer, *Prog. Mater. Sci.*, 2007, **52**, 1263.
3 R. V. Ulijn and A. M. Smith, *Chem. Soc. Rev.*, 2008, **37**, 664; D. N. Woolfson and M. G. Ryadnov, *Curr. Opin. Chem. Biol.*, 2006, **10**, 559.
4 M. G. Ryadnov and D. N. Woolfson, *Nat. Mater.*, 2003, **2**, 329; M. Pechar, P. Kopeckova, L. Joss and J. Kopecek, *Macromol. Biosci.*, 2002, **2**, 199; K. Pagel and B. Koksch, *Curr. Opin. Chem. Biol.*, 2008, **12**, 730.
5 S. Cavalli, F. Albericio and A. Kros, *Chem. Soc. Rev.*, 2010, **39**, 241; H. G. Börner, *Prog. Polym. Sci.*, 2009, **34**, 811; J. Hentschel, M. G. J. ten Cate and H. G. Börner, *Macromolecules*, 2007, **40**, 9224; J. M. Smeenk, M. B. J. Otten, J. Thies, D. A. Tirrell, H. G. Stunnenberg and J. C. M. van Hest, *Angew. Chem., Int. Ed.*, 2005, **44**, 1968; R. J. Williams, A. M. Smith, R. Collins, N. Hodson, A. K. Das and R. V. Ulijn, *Nat. Nanotechnol.*, 2009, **4**, 19.
6 J. D. Hartgerink, T. D. Clark and M. R. Ghadiri, *Chem.–Eur. J.*, 1998, **4**, 1367; J. Couet, J. D. Jeyaprakash, S. Samuel, A. Kopyshev, S. Santer and M. Biesalski, *Angew. Chem., Int. Ed.*, 2005, **44**, 3297; H. A. Lashuel, S. R. LaBrenz, L. Woo, L. C. Serpell and J. W. Kelly, *J. Am. Chem. Soc.*, 2000, **122**, 5262.
7 J. Hentschel and H. G. Börner, *J. Am. Chem. Soc.*, 2006, **128**, 14142; J. Hentschel, E. Krause and H. G. Börner, *J. Am. Chem. Soc.*, 2006, **128**, 7722.
8 D. Eckhardt, M. Groenewolt, E. Krause and H. G. Börner, *Chem. Commun.*, 2005, 2814; H. G. Börner, B. Smarsly, J. Hentschel, A. Rank, R. Schubert, Y. Geng, D. E. Discher, T. Hellweg and A. Brandt, *Macromolecules*, 2008, **41**, 1430.
9 K. Janek, J. Behlke, J. Zipper, H. Fabian, Y. Georgalis, M. Beyermann, M. Bienert and E. Krause, *Biochemistry*, 1999, **38**, 8246.
10 S. Kessel and H. G. Börner, *Macromol. Rapid Commun.*, 2008, **29**, 419.
11 S. Kessel, A. Thomas and H. G. Börner, *Angew. Chem., Int. Ed.*, 2007, **46**, 9023.
12 C. J. Cavender and V. J. Shiner, *J. Org. Chem.*, 1972, **37**, 3567.
13 E. D. Goddard-Borger and R. V. Stick, *Org. Lett.*, 2007, **9**, 3797.
14 W. H. Binder and R. Sachsenhofer, *Macromol. Rapid Commun.*, 2007, **28**, 15; J.-F. Lutz, *Angew. Chem., Int. Ed.*, 2007, **46**, 1018; A. J. Dirks, J. Cornelissen, F. L. van Delft, J. C. M. van Hest, R. J. M. Nolte, A. E. Rowan and F. Rutjes, *QSAR Comb. Sci.*, 2007, **26**, 1200.
15 D. Gebauer, H. Cölfen, A. Verch and M. Antonietti, *Adv. Mater.*, 2009, **21**, 435.
16 D. Gebauer, A. Völkel and H. Cölfen, *Science*, 2008, **322**, 1819.